ORGANOMETALLICS
Article

Organometallics **2010,** *29,* 417–427 417
DOI: 10.1021/om900991b

Rational Design of Highly Cytotoxic η^6-Arene β-Diketiminato−Ruthenium Complexes

Andrew D. Phillips,*[,†,‡] Olivier Zava,[‡] Rosario Scopelitti,[‡] Alexey A. Nazarov,[‡] and Paul J. Dyson*[,‡]

[†]*School of Chemistry and Chemical Biology, University College Dublin, Belfield, Dublin 4, Ireland and* [‡]*Institut des Sciences et Ingénierie Chimiques, Ecole Polytechnique Fédérale de Lausanne (EPFL), CH-1015 Lausanne, Switzerland*

Received November 13, 2009

A series of ruthenium−benzene complexes with β-diketiminate ligands modified with electron-withdrawing groups were prepared and characterized by NMR spectroscopy, mass spectrometry, and single-crystal X-ray diffraction. The complexes are stable in air and undergo controlled hydrolysis in water. The complexes were evaluated for anticancer activity in vitro, and two of them proved to be highly cytotoxic, comparable or even superior to cisplatin. This work shows the potential utility of the β-diketiminate ligand in the rational design of new anticancer metal-containing drugs. A related complex with a η^6-$C_6H_5CF_3$ ligand was prepared and found to undergo a nucleophilic addition reaction at the coordinated arene ring to afford a substituted η^5-cyclohexadienyl derivative.

Introduction

Organometallic compounds are under intensive investigation as putative chemotherapeutic compounds.[1−7] This research is being driven by a continuing search for new types of ligands that endow a metal with specific biological functions while providing relevant stability and pharmacokinetic properties.[8,9] While many different classes of organometallic compounds are under evaluation, the η^6-arene ruthenium complexes have proven to be a highly versatile class of metallopharmaceutical. A number of different types of auxiliary supporting ligands have been used in conjugation with the η^6-arene ligand including water-soluble phosphines, acetylacetones, imidazoles, maltol, ethylenediamines, and others.[10−21] It seems that many different supporting ligands can be used in combination with the ruthenium(II)−arene motif to provide different biological functions, including biologically active ligands,[22−24] and functionalization of the arene is also possible;[25,26] however, at present very few structure−activity relationships have been developed,

*Corresponding authors. E-mail: andrew.phillips@ucd.ie; paul.dyson@epfl.ch.

(1) Jaouen, G. *Bioorganometallics*; VCH-Wiley: Weinheim, 2006.
(2) Hartinger, C. G.; Dyson, P. J. *Chem. Soc. Rev.* **2009**, *38* (2), 391–401.
(3) Allardyce, C. S.; Dorcier, A.; Scolaro, C.; Dyson, P. J. *Appl. Organomet. Chem.* **2005**, *19* (1), 1–10.
(4) Allardyce, C. S.; Dyson, P. J. *Bioorganomet. Chem.* **2006**, *17*, 177–210.
(5) Fish, R. H.; Jaouen, G. *Organometallics* **2003**, *22* (11), 2166–2177.
(6) van Staveren, D. R.; Metzler-Nolte, N. *Chem. Rev.* **2004**, *104* (12), 5931–5986.
(7) Leyva, L.; Sirlin, C.; Rubio, L.; Franco, C.; Lagadec, R. L.; Spencer, J.; Bischoff, P.; Gaiddon, C.; Loeffler, J.-P.; Pfeffer, M. *Eur. J. Inorg. Chem.* **2007**, (19), 3055–3066.
(8) Dyson, P. J. *Chimia* **2007**, *61* (11), 698–703.
(9) Ang, W. H.; Dyson, P. J. *Eur. J. Inorg. Chem.* **2006**, *20*, 4003–4018.
(10) Ferreira, A. P.; da Silva, J. o. L. F.; Duarte, M. T.; da Piedade, M. F. t. M.; Robalo, M. P.; Harjivan, S. G.; Marzano, C.; Gandin, V.; Marques, M. M. *Organometallics* **2009**, *28* (18), 5412–5423.
(11) Peacock, A. F. A.; Melchart, M.; Deeth, R. J.; Habtemariam, A.; Parsons, S.; Sadler, P. J. *Chem.−Eur. J.* **2007**, *13* (9), 2601–2613.
(12) Kandioller, W.; Hartinger, C. G.; Nazarov, A. A.; Kuznetsov, M. L.; John, R. O.; Bartel, C.; Jakupec, M. A.; Arion, V. B.; Keppler, B. K. *Organometallics* **2009**, *28* (15), 4249–4251.
(13) Peacock, A. F. A.; Sadler, P. J. *Chem.−Eur. J.* **2008**, *3* (11), 1890–1899.
(14) Berger, I.; Hanif, M.; Nazarov, A. A.; Hartinger, C. G.; John, R. O.; Kuznetsov, M. L.; Groessl, M.; Schmitt, F.; Zava, O.; Biba, F.; Arion, V. B.; Galanski, M.; Jakupec, M. A.; Juillerat-Jeanneret, L.; Dyson, P. J.; Keppler, B. K. *Chem.−Eur. J.* **2008**, *14* (29), 9046–9057.
(15) Renfrew, A. K.; Phillips, A. D.; Egger, A. E.; Hartinger, C. G.; Bosquain, S. S.; Nazarov, A. A.; Keppler, B. K.; Gonsalvi, L.; Peruzzini, M.; Dyson, P. J. *Organometallics* **2009**, *28* (4), 1165–1172.
(16) Renfrew, A. K.; Phillips, A. D.; Tapavicza, E.; Scopelliti, R.; Rothlisberger, U.; Dyson, P. J. *Organometallics* **2009**, *28* (17), 5061–5071.
(17) Vock, C. A.; Ang, W. H.; Scolaro, C.; Phillips, A. D.; Lagopoulos, L.; Juillerat-Jeanneret, L.; Sava, G.; Scopelliti, R.; Dyson, P. J. *J. Med. Chem.* **2007**, *50* (9), 2166–2175.
(18) Vock, C. A.; Renfrew, A. K.; Scopelliti, R.; Juillerat-Jeanneret, L.; Dyson, P. J. *Eur. J. Inorg. Chem.* **2008**, (10), 1661–1671.
(19) Vock, C. A.; Scolaro, C.; Phillips, A. D.; Scopelliti, R.; Sava, G.; Dyson, P. J. *J. Med. Chem.* **2006**, *49* (18), 5552–5561.
(20) Scolaro, C.; Chaplin, A. B.; Hartinger, C. G.; Bergamo, A.; Cocchietto, M.; Keppler, B. K.; Sava, G.; Dyson, P. J. *Dalton Trans.* **2007**, 5065–5072.
(21) Ang, W. H.; Daldini, E.; Scolaro, C.; Scopelliti, R.; Juillerat-Jeannerat, L.; Dyson, P. J. *Inorg. Chem.* **2006**, *45* (22), 9006–9013.
(22) Schmid, W. F.; John, R. O.; Arion, V. B.; Jakupec, M. A.; Keppler, B. K. *Organometallics* **2007**, *26* (26), 6643–6652.
(23) Schmid, W. F.; John, R. O.; Mühlgassner, G.; Heffeter, P.; Jakupec, M. A.; Galanski, M.; Berger, W.; Arion, V. B.; Keppler, B. K. *J. Med. Chem.* **2007**, *50* (25), 6343–6355.
(24) Ang, W. H.; De Luca, A.; Chapuis-Bernasconi, C.; Juillerat-Jeanneret, L.; Lo Bello, M.; Dyson, P. J. *ChemMedChem* **2007**, *2* (12), 1799–1806.
(25) Ang, W. H.; Daldini, E.; Juillerat-Jeanneret, L.; Dyson, P. J. *Inorg. Chem.* **2007**, *46* (22), 9048–9050.
(26) Ang, W. H.; Parker, L. J.; De Luca, A.; Juillerat-Jeanneret, L.; Morton, C. J.; Lo Bello, M.; Parker, M. W.; Dyson, P. J. *Angew. Chem., Int. Ed.* **2009**, *48* (21), 3854–3857.

Published on Web 12/22/2009

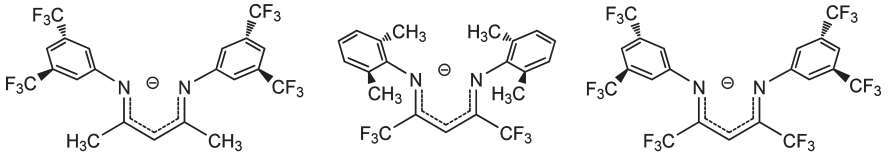

4 **5** **6**

Figure 1. Substitution pattern of the β-diketiminato ligands with electron-withdrawing substituents employed in this study.

Chart 1

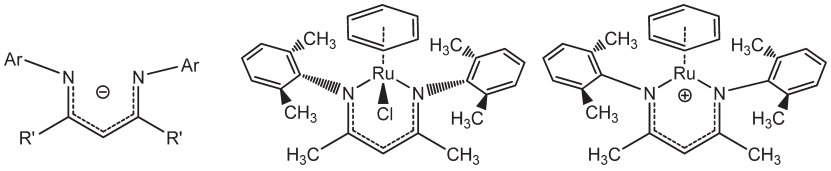

1 **2** **3**

although some trends are emerging. In any case, compared to platinum-based drugs, ligand-based studies are limited, and there is a sustained need for further ligand screening to facilitate a more rational drug design approach.

Recently our research has focused on an interesting family of anionic ligands, namely, the diazo-chelating β-diketiminates **1**, which have traditionally found widespread use in the isolation of a wide variety of unusual and interesting main-group-, lanthanide-, and actinide-centered complexes.[27] Despite a growing number of catalytic applications of metal−β-diketiminate complexes reported in the past decade, as far as we are aware, no biological applications of β-diketiminate-containing complexes have been reported. Instead, within the field of bioinorganic chemistry, the synthesis and characterization of low-coordinate complexes supported by β-diketiminates have focused on the binding of small-molecule substrates in unusual bonding modes, and a number of complexes have been identified as models for the catalytically active sites in metalloenzymes.[28−31]

Previously, we reported the first examples of β-diketiminato−ruthenium complexes that also contain a η^6-C_6H_6 ligand, both with (**2**) and without (**3**) a chloride co-ligand; see Chart 1.[32,33] The bifunctional nature of these compounds proved valuable in metal−ligand-mediated catalysis.[34] Through the rational modulation of the β-diketiminato ligand we report herein on a series of new arene β-diketiminato−ruthenium complexes that display potent in vitro anticancer activity. Indeed, the results lead us to hypothesize that the ability of the β-diketiminato ligand to induce the facile loss of the chloride ligand may facilitate reactions with potential biomolecular targets.

Results and Discussion

A useful feature of β-diketiminate ligands is the ability to modulate their electronic and steric properties by changing the nature of the flanking aryl groups and the substituent at the α-positions of the ligand backbone. Previously, we reported the chloro-β-diketiminato−ruthenium complex **2**, with electron-donating substituents, i.e., 2,6-dimethylphenyl and α-methyl groups, which displays limited stability in solution when exposed to water or oxygen.[32] In order to deter reactivity with O_2 and control the rate of hydrolysis, deactivation of the nucleophilic properties associated with the central β-carbon position of the β-diketiminate ligand is essential. Deactivation may be accomplished by introducing strongly electron-withdrawing CF_3 groups onto the β-diketiminate ligand. Accordingly, three different ligands, **4**, **5**, and **6** (see Figure 1), were synthesized using established literature procedures. Furthermore, a simple unsubstituted β-diketiminate ligand with phenyl flanking groups was prepared as a reference compound to assist in comparing the stability of complexes bearing electron-withdrawing groups. This β-diketiminate was obtained in high yield according to the procedures described by Holm and McGeachin;[35,36] however, decomposition is observed if this compound is not protected from moisture. Ligand **4** was prepared under conditions similar to those used for 2,6-dimethylphenyl-substituted β-diketiminate. The synthesis of ligand **5** relied on titanium chloride-assisted thermocoupling of substituted anilines with hexafluoroacetylacetone as described previously,[37,38] whereas compound **6** utilized the thermal-induced method of N=C coupling, using the ylid $Ph_3P{=}N(3,5\text{-}(CF_3)_2C_6H_3)$ and $CF_3C(O)CH_2C(O)CF_3$, with elimination of Ph_3PO as described by Sadighi.[39]

To facilitate binding of the β-diketiminate ligand to the η^6-arene−ruthenium fragment, deprotonation of the azo center was accomplished using *n*-butyllithium in hydrocarbon

(27) Bourget-Merle, L.; Lappert, M. F.; Severn, J. R. *Chem. Rev.* **2002**, *102* (9), 3031–3066.
(28) Holland, P. L. *Can. J. Chem.* **2005**, *83* (4), 296–301.
(29) Tolman, W. B., Ed. *Activation of Small Molecules: Organometallic and Bioinorganic Perspectives*; 2006; p 363.
(30) Tolman, W. B.; Spencer, D. J. E.; Reynolds, A. M.; Holland, P. L.; Jazdzewski, B. A.; Young, V. G. *J. Inorg. Biochem.* **2001**, *86* (1), 107–107.
(31) Inosako, M.; Kunishita, A.; Shimokawa, C.; Teraoka, J.; Kubo, M.; Ogura, T.; Sugimoto, H.; Itoh, S. *Dalton Trans.* **2008**, *44*, 6250–6256.
(32) Phillips, A. D.; Laurenczy, G.; Scopelliti, R.; Dyson, P. J. *Organometallics* **2007**, *26* (5), 1120–1122.
(33) Moreno, A.; Pregosin, P. S.; Laurenczy, G.; Phillips, A. D.; Dyson, P. J. *Organometallics* **2009**, *28* (22), 6432−6441.
(34) Grützmacher, H. *Angew. Chem., Int. Ed.* **2008**, *47* (10), 1814–1818.
(35) McGeachin, S. G. *Can. J. Chem.* **1968**, *46* (11), 1903–1912.
(36) Parks, J. E.; Holm, R. H. *Inorg. Chem.* **1968**, *7* (7), 1408–1416.
(37) Carey, D. T.; Cope-Eatough, E. K.; Vilaplana-Mafe, E.; Mair, F. S.; Pritchard, R. G.; Warren, J. E.; Woods, R. J. *Dalton Trans.* **2003**, *6*, 1083–1093.
(38) Li, Y.; Jiang, L.; Wang, L.; Gao, H.; Zhu, F.; Wu, Q. *Appl. Organomet. Chem.* **2006**, *20* (3), 181–186.
(39) Laitar, D. S.; Mathison, C. J. N.; Davis, W. M.; Sadighi, J. P. *Inorg. Chem.* **2003**, *42* (23), 7354–7356.

Scheme 1. General Synthetic Route for the η^6-Arene β-Diketiminato−Ruthenium Complexes 7−10

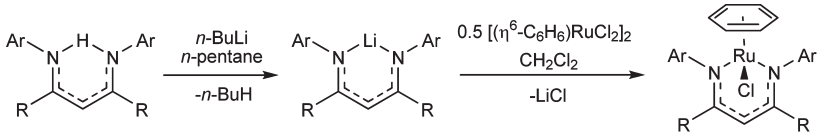

Ar = C_6H_5, R = CH_3
4-H Ar = 3,5-$(CF_3)_2C_6H_3$, R = CH_3
5-H Ar = 2,6-$(CH_3)_2C_6H_3$, R = CF_3
6-H Ar = 3,5-$(CF_3)_2C_6H_3$, R = CF_3

Ar = C_6H_5, R = CH_3
4-Li Ar = 3,5-$(CF_3)_2C_6H_3$, R = CH_3
5-Li Ar = 2,6-$(CH_3)_2C_6H_3$, R = CF_3
6-Li Ar = 3,5-$(CF_3)_2C_6H_3$, R = CF_3

7 Ar = C_6H_5, R = CH_3
8 Ar = 3,5-$(CF_3)_2C_6H_3$, R = CH_3
9 Ar = 2,6-$(CH_3)_2C_6H_3$, R = CF_3
10 Ar = 3,5-$(CF_3)_2C_6H_3$, R = CF_3

solvent at −78 °C to prevent possible decomposition. The resulting β-diketiminato−lithium complexes precipitated from solution;[40] see Scheme 1. We have previously reported the synthesis of the arene chloro-β-diketiminato−ruthenium complex **2**, in which the corresponding β-diketiminato−lithium conjugate is added to the $[(\eta^6\text{-}C_6H_6)RuCl_2]_2$ dimer in dichloromethane and subsequent recrystallization affords the product.[32] Following this procedure, complexes **7**−**10** were prepared in moderate to high yield. Complexes **8**−**10** are air stable, and evidence for decomposition in a saturated dichloromethane solution was detectable by ^{19}F NMR only after several weeks of storage without precautions to exclude air. In contrast, the phenyl-substituted complex **7** displays significantly increased reactivity toward oxygen and water, and manipulation of this compound required the use of inert conditions.

Previously, we have shown that ruthenium complexes bearing fluorinated η^6-arenes can markedly alter the rate of hydrolysis in aqueous solutions.[16] Therefore, in an attempt to isolate a β-diketiminato−ruthenium complex bearing an electron-withdrawing η^6-$C_6H_5CF_3$ arene using the above-mentioned procedure, an unexpected side reaction was observed. The resulting product **11**, obtained in 42% yield, featured two sets of aryl-imine-type resonances in the ^1H NMR spectrum. The structure of **11** was established by X-ray crystallography, revealing the presence of a β-diketiminato−ruthenium moiety; however, a β-diimine ligand was attached through the β-carbon to the para-position of the η^6-arene of species **12** in Scheme 2, forming a compound bearing an anionic η^5-cyclohexadienyl ligand, which is very rare for ruthenium.[41−45] Presumably, the reaction proceeds via nucleophilic attack by the β-carbon position of the β-diketiminato−lithium conjugate, and similar reactions of this type of lithium complex with other substrates have been reported.[37,46] Accordingly, the intermediate precursor of **13** features two anionic ligands, and hence the chloride ligand is eliminated as LiCl, forming **11**. Nucleophilic addition to

Scheme 2. Proposed Mechanism for the Formation of Complex 11, Involving Initial Nucleophilic Attack by the β-Carbon Position of a β-Diketiminato−Lithium Conjugate on the Coordinated η^6-Arene of the Chloro-β-diketiminato−Ruthenium Complex 12, Followed by Elimination of LiCl from 13, Yielding Complex 11, Which Features a Hybrid β-Diimine-η^5-cyclohexadienyl Ligand

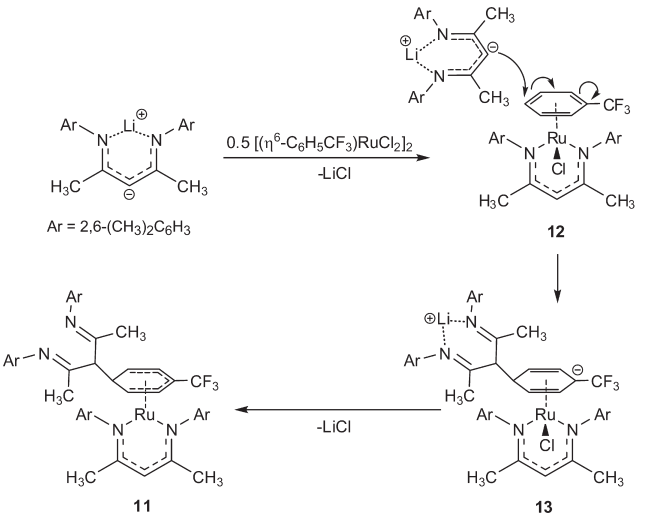

coordinated η^6-arene ligands has been observed for other types of ruthenium complexes.[41−43,47,48]

All the complexes are soluble in chlorinated solvents, methanol, acetone, and DMSO and are slightly soluble in water. The structures of the complexes were confirmed by solution ^1H, ^{13}C, and ^{19}F NMR spectroscopy, and conclusive assignment of all resonances was performed using 2D NMR techniques (gCOSY, HSQC, and HMBC). In the case of the fluorinated compounds, 1D $^{13}C\{^{19}F\}$ NMR spectroscopy was used to simplify the spectra by suppressing the C−F coupling, which otherwise resulted in overlapping quartets. Table 1 lists the various chemical shift values for diagnostic protons and carbons related to the η^6-arene and β-diketiminate ligands. For complex **2**, the ortho-methyl groups are inequivalent, indicating that the aryl group is not able to rotate freely about the C_{ipso}−N bond. In **9**, however, the ortho-methyl group resonances are observed as a broad singlet ($w_{1/2}$ = 30 Hz), and although rotation of the aryl group is sterically restricted, the origin of this dynamic behavior probably results in a dynamic bending of the β-diketiminate ligand along the N,N′-vector. Moreover,

(40) Stender, M.; Wright, R. J.; Eichler, B. E.; Prust, J.; Olmstead, M. M.; Roesky, H. W.; Power, P. P. *J. Chem. Soc., Dalton Trans.* **2001**, *23*, 3465–3469.
(41) Robertson, D. R.; Robertson, I. W.; Stephenson, T. A. *J. Organomet. Chem.* **1980**, *202* (3), 309–318.
(42) Robertson, D. R.; Stephenson, T. A. *J. Organomet. Chem.* **1977**, *142* (2), C31–C34.
(43) Bhambri, S.; Tocher, D. A. *J. Organomet. Chem.* **1996**, *507* (1−2), 291–293.
(44) Yang, S.-M.; Chan, M. C.-W.; Peng, S.-M.; Che, C.-M. *Organometallics* **1998**, *17* (2), 151–155.
(45) Huckett, S. C.; Angelici, R. J. *Organometallics* **2002**, *7* (7), 1491–1500.
(46) Burford, N.; D'Eon, M.; Ragogna, P. J.; McDonald, R.; Ferguson, M. J. *Inorg. Chem.* **2004**, *43* (2), 734–738.
(47) Le Bozec, H.; Touchard, D.; Dixneuf, P. H. *Organometallic Chemistry of Arene Ruthenium and Osmium Complexes*; Academic Press: London, 1989; Vol. *29*, pp 163−248.
(48) Bennett, M. A. *Coord. Chem. Rev.* **1997**, *166*, 225–254.

Table 1. Selected ^{1}H and ^{13}C NMR Chemical Shifts of the η^6-C_6H_6 and β-Diketiminate Ligands in 2 and 7−10

	aryl	R	$\delta(^1H)$ β-C*H*	$\delta(^{13}C)$ β-*C*H	$\delta(^{13}C)$ α-*C*CH_3	$\delta(^1H)$ C_6H_6	$\delta(^{13}C)$ C_6H_6	$\delta(^{19}F)$ Ar−CF_3	$\delta(^{19}F)$ α-CF_3
2	2,6-$Me_2C_6H_3$	Me	5.77	99.53	160.81	4.84	85.38		
7	C_6H_5	Me	4.45	94.42	159.85	4.52	86.32		
8	3,5-$(CF_3)_2C_6H_3$	Me	4.45	94.41	160.10	4.52	86.30	−59.2	
9	2,6-$Me_2C_6H_3$	CF_3	5.52	90.93	151.35	4.57	87.93		−64.2
10	3,5-$(CF_3)_2C_6H_3$	CF_3	5.54	86.90	150.85	4.67	87.49	−63.3	−59.7

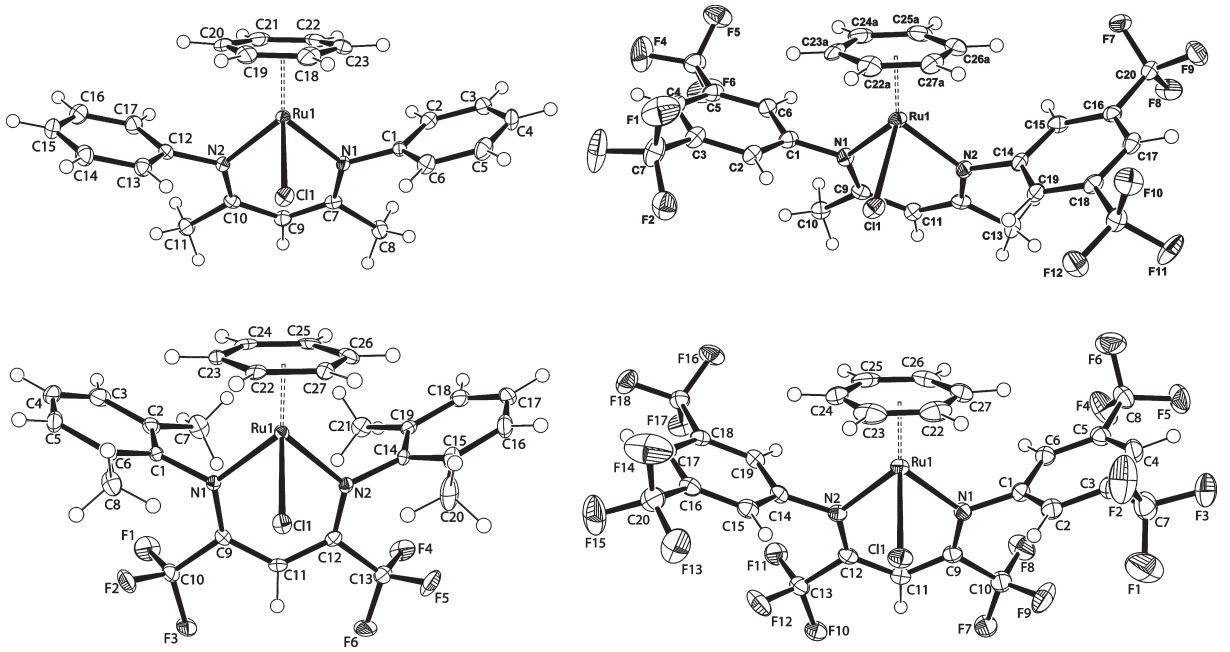

Figure 2. ORTEP diagrams of **7** (top left), **8** (top right), **9** (bottom left), and **10** (bottom right). Thermal ellipsoids are drawn with 50% probability. Solvates and η^6-C_6H_6 disorder have been omitted for clarity.

the fluorine atoms of the α-CF_3 group also exhibit broadening in the ^{19}F NMR spectrum (see below). In contrast, complexes **8** and **10** with CF_3-substitution on the 3- and 5-positions of the flanking aryl groups feature only a single resonance in the ^{19}F NMR spectra with the equivalence being due to free rotation about the N−C_{ipso} bond.

A comparison of the NMR data of **2** with **7** reveals considerable electronic differences between the two compounds. In particular, the $\delta(^1H)$ and $\delta(^{13}C)$ of the β-CH position are more deshielded in **2**, suggesting a greater buildup of electron density in this region of the β-diketiminate ligand. The structural dichotomy between the complexes is strongly evident in the solid-state structure (see below). Moreover, the $\delta(^1H)$ and $\delta(^{13}C)$ values associated with the η^6-C_6H_6 ring provide an indication of the relative strength of metal−benzene bonding in the series of complexes and importantly the influence exerted by different β-diketiminate ligands; complex **2**, with the most strongly donating ligand of the series, has a η^6-benzene with the highest amount of distortion in planarity, as shown by a more shielded $\delta(^1H)$ value. In contrast, the fluorinated β-diketiminate complexes, especially those with CF_3 α-substitution, i.e., **8** and **10**, have the least distorted η^6-C_6H_6 ring, suggesting relatively weak σ-donation by these electron-withdrawing β-diketiminato ligands.

Complexes **7**−**10** were analyzed by ESI-MS in the positive ion mode in CH_2Cl_2 or MeOH, which in general afforded a strong peak envelope corresponding to the molecular species in which the chloride ligand and a proton had been lost, viz., $[M - Cl - H]^+$. Fragmentation of the $[M - Cl - H]^+$ peak by collision-induced dissociation (CID) revealed that the η^6-benzene ligand is lost in preference to the β-diketiminate ligand. Further fragmentation did not result in loss of the β-diketiminate ligand, but instead at high CID energies, loss of the flanking aryl groups was observed. The ESI-MS for the phenyl-substituted complex **7** also revealed an additional peak at 16 m/z greater than the cationic parent ion, 429.0 m/z. This species features a single oxygen, presumably bound to the Ru center, as observed in a number of reported ruthenium porphyrin species.[49,50] Furthermore, if the ESI-MS is performed with degassed solvent, this additional signal is suppressed. Only **2** and **7** demonstrated this behavior; species bearing electron-withdrawing groups in the aryl or α-position showed no indication of a Ru−O containing species.

Structural Characterization of 7−11 in the Solid State. Suitable single crystals of **7**−**10** were obtained using solvent diffusion methods (see Experimental Section) and were analyzed by X-ray diffraction, and the resulting structures are shown in Figure 2. All complexes have a piano-stool-type geometry with the Cl−Ru vector bisecting the chelating β-diketiminate ligand, with the latter bond being parallel to the β-CH position. A comparison of the pertinent bonding parameters for the complexes reveals that the most striking difference concerns the Ru−Cl bond length. Previously we

(49) Meunier, B. *Chem. Rev.* **2002**, *92* (6), 1411–1456.
(50) Groves, J. T.; Shalyaev, K.; Lee, J. *Oxometalloporphyrins in Oxidative Catalysis*; Academic Press: London, 2000; Vol. *4*, pp 17−40.

Table 2. Selected Bond Lengths (Å) and Angles (deg) for Complexes 2 and 7−10

	2	7	8[a]	9[a]	10
Ru−Cl	2.521(1)	2.461(1)	2.464(2)	2.463(1)	2.414(1)
Ru−N	2.099(2)	2.105(2)	2.115(5)	2.127(2)	2.108(2)
		2.102(2)	2.103(4)	2.115(2)	2.106(2)
C_{ipso}−N	1.450(4)	1.440(3)	1.431(7)	1.460(4)	1.436(3)
		1.439(3)	1.435(7)	1.457(3)	1.433(3)
N−C_α	1.335(3)	1.330(3)	1.332(7)	1.326(3)	1.319(3)
		1.330(4)	1.335(7)	1.323(3)	1.314(3)
C_α−C_β	1.394(3)	1.398(4)	1.398(8)	1.400(4)	1.391(3)
		1.406(4)	1.395(7)	1.394(4)	1.391(3)
C_α−C(H/F)$_3$	1.518(4)	1.525(4)	1.525(8)	1.533(4)	1.530(3)
		1.522(4)	1.529(7)	1.536(4)	1.537(3)
Ru−arene[b]	1.687(1)	1.690(13)	1.715(4)	1.673(5)	1.703(1)
			1.672(6)	1.734(7)	
arene[b]−Ru−Cl	122.3(1)	125.6(1)	123.2(1)	122.8(2)	126.0(1)
			129.1(1)	127.1(3)	
arene[b]−Ru−N[c]	154.1(1)	150.7(8)	153.2(2)	155.5(2)	154.0(1)
			147.3(2)	151.2(3)	
Cl−Ru−N[c]	83.6(1)	83.5(1)	83.5(1)	81.7(1)	80.0(1)
N−Ru−N	86.6(1)	88.5(1)	88.3(3)	88.1(1)	87.8(1)
C_{ipso}−N−Ru	118.5(2)	115.0(2)	114.5(3)	118.2(2)	113.8(1)
		115.0(2)	115.6(3)	116.8(2)	113.5(1)
C_{ipso}−N−C_α	116.8(2)	118.3(2)	118.4(4)	119.0(2)	120.0(2)
		118.0(2)	117.5(4)	120.7(2)	120.4(2)
N−C_β−C_α	118.9(2)	119.2(2)	120.0(5)	119.3(2)	126.1(2)
		120.5(2)	119.2(5)	119.0(2)	126.4(2)
C_α−C_β−C_α	126.8(3)	128.6(3)	129.5(5)	126.0(3)	126.6(2)
Ru−N[c]−C_α	157.8(2)	178.2(1)	177.3(3)	155.1(1)	170.5(1)

[a] The η^6-C_6H_6 ring is disordered between two sites in these complexes. [b] Refers to the centroid position of the η^6-C_6H_6 ligand. [c] Refers to the midpoint of the vector connecting both nitrogen centers.

have reported that **2** features the longest Ru−Cl bond for all known η^6-arene ruthenium-containing complexes.[32] The weakness of this bond is confirmed by facile removal or substitution of the chloride ligand. The other newly reported complexes feature significantly shorter Ru−Cl distances and average about 2.46 Å, which is close to the median value reported for all compounds featuring the η^6-arene−Ru fragment in the CSD,[51] except for the highly substituted fluorinated complex **10**, which has the shortest Ru−Cl bond of the series reported in this paper. The Ru−N and Ru−C(arene) distances are largely consistent across the series and do not change significantly with different β-diketiminate substitution patterns. Within the β-diketiminato ligand structure bond distances and angles are also invariant, as indicated by identical N−C_α bond lengths and C_α−C_β−C_α bond angles; see Table 2.

Two distinctive geometric forms are observed in the structures, which are typified by **2** and **9**; see Figures 2 and 3. In complexes featuring ortho-positioned methyl flanking aryls, **2** and **9**, folding occurs in the β-diketiminate ligand along the N−N vector. This folding effectively divides and separates the π-bonding of the chelating ligand into two distinctive regions, N−Ru−N and C_α−C_β−C_α. A folding of the flanking aryl groups toward the benzene ligand ensures that both nitrogen atoms are planar and engaged in π-bonding. The tilting angle of the aza groups toward the Ru center indicates this π-delocalized allylic-type interaction involves the metal d-orbitals. Moreover, the orientation of the η^6-benzene is orthogonal to the central β-diketiminate ligand plane. The N,N′ ligand folding in **2** and **9** is exemplified by the narrower Ru−$N_{centriod}$−C_α angles of approximately 150° compared to ca. 180° in **7**, **8**, and **10**, indicative of a completely planar β-diketiminate ligand incorporating the metal center. Consequently, the η^6-benzene is tilted in the opposite direction away from the chloride ligand, and the Ru−Cl bond vector is almost at a right angle with the ligand plane. This type of geometry is very similar to that observed in η^6-arene chloro-acetylacetone complexes featuring ruthenium.[52]

Complex **9**, with α-CF_3 groups, adopts folded β-diketiminate geometry, but in solution, there appears to be a rapid equilibrium between both types of ligand geometries, as exemplified by complexes **2** and **7**; see Figure 3. Interestingly, all of the complexes retain near identical Cl−Ru−N_β bond angles (see Table 2). The ortho-CH_3 substitution on the flanking aryls in **9** also promotes a repulsive steric effect, which is demonstrated by wider Ru−N−C_{ipso} angles compared to **7**, **8**, and **10**. A stronger steric effect is observed in the α-substitution of the CF_3 versus CH_3 group in the β-diketiminate ligand. Specifically, the C_α−C(F_3) bonds in **9** and **10** are longer than the corresponding C_α−C(H_3) bonds in **2**, **7**, and **8**. This is somewhat counterintuitive, since it is expected that the strongly electron withdrawing groups should shorten bonds and enhance the transfer of electron density. However, it is apparent that the repulsive steric effects of the larger size fluorine are dominant, and thus the group as a whole imparts a greater ionic polar component to the C−CF_3 bond, i.e., δ^+C—$\delta^-$$CF_3$.[53] A comparison of **2** and **9** with ortho-methyl substitution (see Figure 2) reveals that the most significant changes are larger N−C_α−C(H/F) bond angles and a slight decrease in the Ru−N−C_{ipso} bond angle in **9**. All these features can be traced to greater repulsive effects of the trifluoromethyl group. Further discussion regarding the solid-state characterization of complexes **7**−**10** is given in the Supporting Information.

The structure of **11** is shown in Figure 4, with selected structural parameters given in Table 3. The β-diketiminato−ruthenium fragment has metric parameters that are identical to those of the cationic η^6-arene β-diketiminato−ruthenium species, **3**, previously described.[33] The Ar−N═C(CH_3) (Ar = 2,6-dimethylphenyl) arms of the β-diimine-η^6-cyclohexadienyl ligand are disordered over two sites, with the common linkage site being the β-carbon, which is attached to the η^6-cyclohexadienyl moiety. The elongated N−C bonds have distances that are consistent with imine-type bonds. The η^6-cyclohexadienyl ligand consists of a methylene CH_2 group, which is puckered away from the metal center; however, this particular ligand is more highly distorted than the η^6-C_6H_7 ligand found in the ruthenium-1,4,7-triazacyclononane complex, which is probably due to the presence of the highly electron withdrawing CF_3 and β-diimine groups.

Computational Analysis of 2 and 7−10. Density functional theory was used to optimize structures **7**−**10** to an energetic minimum, and vibration analysis confirmed that the structures were the lowest points on the local potential energy surface. Geometrical comparison indicated that all calculated structures have overestimated bond distances as compared to the experimentally observed distances in the solid state, cf. Tables 2 and 3. However, these results are typical for

(51) Allen, F. *Acta Crystallogr. Sect. B* **2002**, *58* (3 Part 1), 380–388.

(52) Habtemariam, A.; Melchart, M.; Fernandez, R.; Parsons, S.; Oswald, I. D. H.; Parkin, A.; Fabbiani, F. P. A.; Davidson, J. E.; Dawson, A.; Aird, R. E.; Jodrell, D. I.; Sadler, P. J. *J. Med. Chem.* **2006**, *49* (23), 6858–6868.

(53) Crampton, M. R.; Emokpae, T. A.; Isanbor, C. *Eur. J. Org. Chem.* **2007**, (8), 1378–1383.

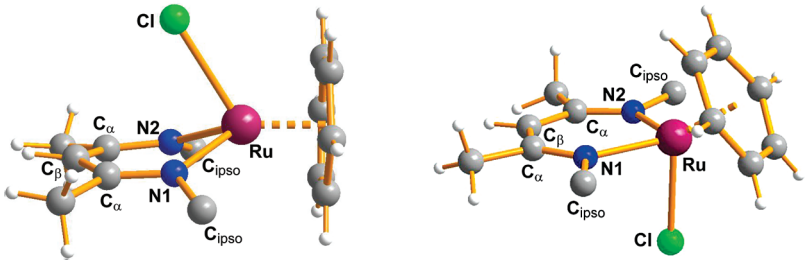

Figure 3. Comparison of the two major structural variants observed. Complexes with the 2,6-dimethylphenyl flanking aryl groups, **2** and **9** (left), feature a fold along the N,N′ vector and divide the β-diketiminate into two regions. Compounds **7**, **8**, and **10** have no ortho substitution on the flanking aryl (right) and feature a planar β-diketiminate ligand including the Ru center. Also these complexes contain a tilted η^6-arene group, while complexes **2** and **9** (left) have a perpendicular-oriented arene.

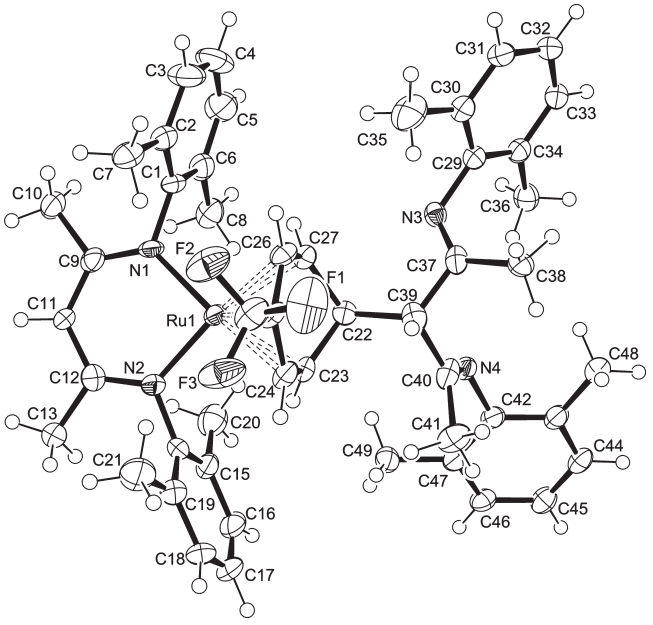

Figure 4. ORTEP diagram of **11** with thermal ellipsoids drawn with 50% probability. The disorder associated with the η^5-cyclohexadienyl β-diimine ligand has been omitted for clarity.

geometry optimizations that employ the hybrid functional BYL3P.[54,55] Importantly, the calculated structures reproduce accurately the observed structural trends between the different complexes, including the Ru−Cl and Ru−N bond lengths and the ruthenium−η^6-arene centroid distances; see Table 4. A comparison of the calculated and observed structures for all the complexes is provided in the Supporting Information, Figures S4−S7. For each system, the Mayer bond indices (MBI) for selected diagnostic bonds within the complexes were calculated and give a useful indication of the relative bond strengths among the series (see Table 4). The MBI values highlight a number of trends among the complexes, specifically for **10**, featuring the heavily fluorinated β-diketiminate ligand. In agreement with the observed solid-state Ru−Cl bond distances, **10** has the shortest and strongest Ru−Cl bond of the series. However, the MBI values also reveal that **10** has the weakest metal coordination to the η^6-benzene. Conversely, **2**, which has the strongest electron donating β-diketiminate ligand, as indicated by strong metal binding, i.e., MBI(Ru−N) = 0.503, also has the most strongly bound η^6-benzene of the series. This result is consistent with the established bonding model of η^6-arenes with metal centers, where a stronger electron donation into the π^* MOs of the arene induces a greater π-back-bonding interaction with the coordinated metal.

The calculated models also provided useful information regarding the nucleophilicity of the β-carbon atom. Our impetus for employing the fluorinated β-diketiminate ligand was to deter reactivity with oxygen to prevent complex deactivation. Previous work has demonstrated that the cationic complex **2** promotes heterolytic cleavage of H_2 through a cooperative binding of the metal and β-carbon position. Therefore, assuming a similar reactivity of η^6-arene β-diketiminato−ruthenium with dioxygen, reducing the charge of the β-carbon position is essential for obtaining stability in a physiological environment. By introducing electron-withdrawing groups to the β-diketiminate, inductive σ-based mesomeric effects should remove electron density from the central core section of the ligand, including the β-carbon site. To test this assumption, for each complex an electrostatic potential map was generated using a fixed electric-static charge range; see Figure 5. As predicted, the total atomic charge, calculated by the natural bonding order method (NBO), of both the Cl atom and the β-carbon position is reduced with trifluoromethyl substitution irrespective of the substitution pattern of the β-diketiminate; see Table 4. Moreover, replacing CF_3 by CH_3 at the α-positions of the β-diketiminate ligand is more effective at removing electron density from the β-carbon position than using aryl groups with meta-substituted CF_3 groups. However, from the ESP map (see Figure 5), strengthening of the Ru−Cl bond is predicted when the flanking aryl groups contain strongly electron withdrawing groups. This effect is additive, and consequently **10** has the least electronegative Cl and β-carbon center.

Biological Evaluation of 8−10. Prior to the in vitro biological evaluation of **8**−**10** their aqueous stability was studied. Related ruthenium−arene complexes with chelating N- and O-donor ligands have been shown to undergo exchange of the chloride ligand with a water ligand with the rate of this process depending on the electronic nature of the chelating ligand and the reaction conditions (pH, chloride concentration, etc).[11,56] Moreover, for clinically used Pt-based drugs

(54) Sholl, D. S.; Steckel, J. A., *Density Functional Theory: A Practical Introduction*; John Wiley & Sons: Hoboken, NJ, 2009.
(55) Koch, W.; Holthausen, M. C., *A Chemist's Guide to Density Functional Theory*, 2nd ed.; Wiley-VCH: Weinheim, 2001.

(56) Mendoza-Ferri, M. G.; Hartinger, C. G.; Mendoza, M. A.; Groessl, M.; Egger, A. E.; Eichinger, R. E.; Mangrum, J. B.; Farrell, N. P.; Maruszak, M.; Bednarski, P. J.; Klein, F.; Jakupec, M. A.; Nazarov, A. A.; Severin, K.; Keppler, B. K. *J. Med. Chem.* **2009**, *52* (4), 916–925.

Table 3. Selected Bond Distances (Å) and Angles (deg) for 11

N(1)−Ru(1) = 2.050(5)	N(3B)−C(37B) = 1.38(5)	C(39)−C(37B)−N(3B) = 125(3)
N(2)−Ru(1) = 2.054(6)	N(3B)−C(36B) = 2.91(5)	C(38)−C(37)−N(3) = 127.6(11)
N(1)−C(1) = 1.460(9)	N(3B)−C(29B) = 1.41(4)	C(38B)−C(37B)−N(3B) = 107(3)
N(2)−C(14) = 1.447(10)	C(40)−N(4B) = 1.37(4)	C(38)−N(3)−C(29) = 87.4(5)
N(1)−C(9) = 1.340(10)	N(4B)−C(42B) = 1.45(3)	C(38B)−N(3B)−C(29B) = 92.2(18)
N(2)−C(12) = 1.343(10)	N(1)−Ru(1)−N(2) = 88.5(2)	C(39)−C(40)−N(4) = 119.3(7)
C(9)−C(11) = 1.390(10)	C(1)−N(1)−Ru(1) = 116.8(4)	C(39)−C(40)−N(4B) = 109.9(14)
C(11)−C(12) = 1.398(10)	C(14)−N(2)−Ru(1) = 116.6(4)	C(40)−N(4)−C(42) = 123.7(9)
Ru(1)−C(23) = 2.205(6)	Ru(1)−N(1)−C(9) = 127.2(4)	C(40)−N(4B)−C(42B) = 110(2)
Ru(1)−C(24) = 2.166(7)	Ru(1)−N(2)−C(12) = 127.7(5)	C(41)−N(4)−C(42) = 91.8(6)
Ru(1)−C(25) = 2.120(7)	N(1)−C(9)−C(10) = 119.4(6)	C(41B)−N(4B)−C(42B) = 90.4(19)
Ru(1)−C(26) = 2.157(7)	N(2)−C(12)−C(13) = 119.8(7)	
Ru(1)−C(27) = 2.233(7)	N(1)−C(9)−C(11) = 124.7(6)	
C(40)−N(4) = 1.229(12)	N(2)−C(12)−C(11) = 123.7(7)	
C(37)−N(3) = 1.236(14)	C(39)−C(37)−N(3) = 117.2(10)	

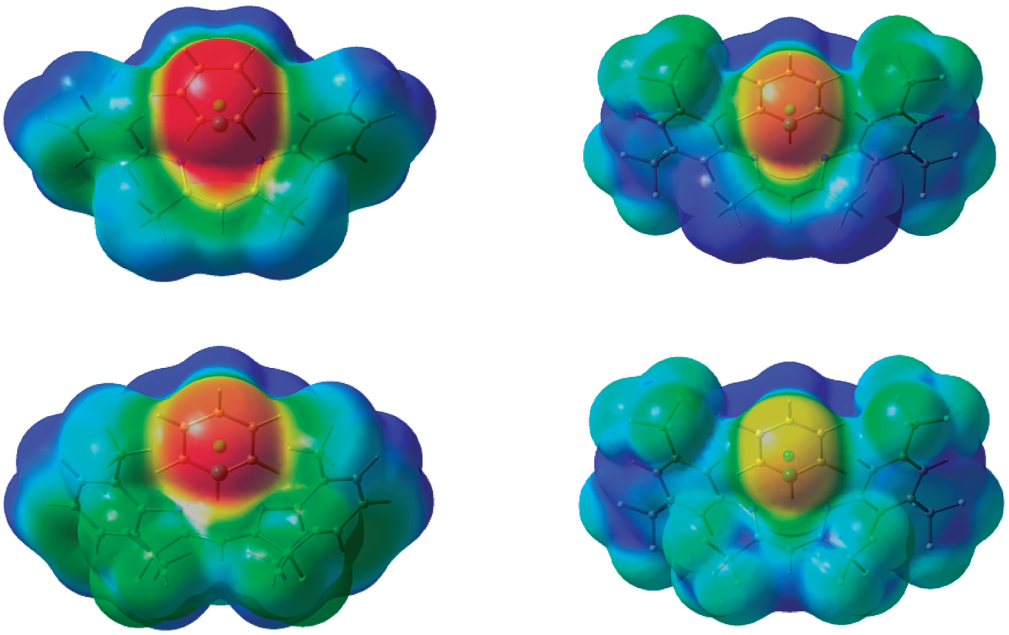

Figure 5. Graphical comparison of the calculated electrostatic potential (ESP) of complexes **7** (top left), **8** (top right), **9** (bottom left), and **10** (bottom right). Each of the 3D ESP maps is drawn with a fixed charge range, where red represents the areas of highest electronegativity and blue represents areas of lowest electronegativity.

Table 4. Comparison of Calculated Ru−Cl, Ru−N, and Ru−C-(η^6-C_6H_6) Bond Distances, along with the Associated Bond Strength, as Indicated by the Mayer Bond Indices (MBI) for Energy-Minimized Gas Phase Complexes 2 and 7−10[a]

		2	7	8	9	10
Ru−Cl (Å)	calc	2.483	2.462	2.449	2.464	2.438
	expt	2.521(1)	2.461(1)	2.464(2)	2.463(1)	2.414(1)
MBI(Ru−Cl)		0.788	0.802	0.829	0.82	0.86
Ru−N (Å)	calc	2.13	2.109	2.118	2.138	2.122
	expt	2.099(2)	2.105(2)	2.115(5)	2.127(2)	2.108(2)
			2.102(2)	2.103(4)	2.115(2)	2.106(2)
MBI		0.509	0.504	0.494	0.497	0.483
Ru−C[b] (Å)	calc	1.804	1.816	1.823	1.819	1.842
	expt	1.687(1)	1.69(1)	1.715(3)[c]	1.673(5)[c]	1.703(1)
				1.672(5)[c]	1.734(7)[c]	
MBI(Ru−C[b])		0.44	0.421	0.423	0.433	0.413
C_β (NBO)		−0.421	−0.431	−0.423	−0.405	−0.411
Cl (NBO)		−0.412	−0.4	−0.374	−0.37	−0.355

[a] The charge of the β-carbon position of the β-diketiminate ligand of the complexes is given, determined by the natural bond order (NBO) method. [b] Refers to the distance between Ru and the centroid point of the η^6-C_6H_6 arene. [c] Experimental accuracy is reduced due to positional disorder of the η^6-C_6H_6 arene.

hydrolysis is believed to be critical for biological activity, although for ruthenium(II)−arene systems direct reaction involving an associative pathway is also possible.[8] Thus, the hydrolysis of **8**−**10** (**7** was not included in this study due to instability; see above) was studied by UV−vis spectrophotometry and ^{1}H NMR spectroscopy. The study shows that in the three complexes the chloride ligand is exchanged by water quite rapidly (< 1 h). Over longer periods the η^6-C_6H_6 ligand may also be displaced. This observation is in agreement with the ESI-MS study (see above) that showed loss of chloride, followed by loss of the benzene (at modest collision energies) without loss of the β-diketiminato ligand observed (even at high collision energies).

The cytotoxicities of **8**−**10**, and cisplatin included as a control, were established on ovarian cancer cells, grown for three days at 37 °C in the presence of the complexes, and following incubation, cell survival was monitored using the MTT assay; see Table 5 and Figure 6. Compound **8** is only sparingly cytotoxic, whereas **9** and **10**, with α-CF_3 substitution in the β-diketiminate backbone, are highly cytotoxic compounds. Their cytotoxicity is equivalent, if not slightly

Table 5. IC_{50} Values (μM) of Compounds 8−10 and Cisplatin Tested on A2780 and A2780cisR Ovarian Cancer Cells

complex	A2780	A2780cisR
8	91 (±3)	108 (±3)
9	1.8 (±0.3)	1.9 (±0.5)
10	< 0.5	< 0.5
cisplatin	4.3 (±0.5)	18.2 (±1)

superior to cisplatin in the A2780 cell line and markedly more effective than cisplatin in the cisplatin-resistant A2780cisR variant.

Indeed, complexes **9** and **10** are among the most active ruthenium−arene compounds reported to date. While comparison should be taken with caution, due to the intrinsic variance between cells (even within the same cell line), most ruthenium−arene compounds tend to be at least an order of magnitude less cytotoxic than **9** and **10**.[2] The increased cytotoxicity may be correlated with the presence of CF_3 groups, with **9** containing α-CF_3 groups on the β-diketiminate ligand and the most cytotoxic compound (IC_{50} < 0.5 μM), i.e., **10**, having α-CF_3 groups and CF_3 groups at the 3,5-positions of the flanking aryl rings. It is unlikely that the increased cytotoxicity emanates from the release of the β-diketiminate ligand, with the ligand being the cytotoxic fragment since loss of the β-diketiminate ligand has not been observed under any conditions. Moreover, the free β-diketiminate ligands are highly insoluble in water, and it was not possible to determine their in vitro activity. Therefore, if the β-diketiminate ligand is released, then this process only occurs once the complex has penetrated the cell membrane.

Concluding Remarks. Modification of the β-diketiminate ligand with electron-withdrawing groups provides oxygen-stable ruthenium(II)−arene complexes that hydrolyze in a controlled fashion when dissolved in water. On the basis of considerable interest in the cytotoxic properties of organometallic compounds,[2,57−64] and in particular of ruthenium(II)−arene half-sandwich complexes,[15−17,19,22,52,65] the β-diketiminato complexes were evaluated for anticancer activity in vitro. Two of these compounds proved to be highly cytotoxic, comparable or even superior to cisplatin. Such strong cytotoxicity is, as far as we are aware, unprecedented for this class of compounds. While further rational modification of the β-diketiminate structure is required, together with further biological studies, this work shows the potential utility of this ligand in the rational design of new anticancer metal-containing drugs.

Experimental Section

Synthesis of the starting materials and complexes was carried out under a purified N_2 atmosphere with standard Schlenk techniques,[66] and manipulations of complexes **2** and **7** were performed in a drybox with a N_2 atmosphere containing less than 1 ppm of O_2 and H_2O. Complexes **8**−**10** could be handled in air without decomposition. All solvents were dried by passage through aluminum oxide columns or, in some cases, degassed by passage through a copper column (Innovative Technologies) and then stored in Schlenk flasks. Celite (545 grade, Merck Co.) was dried at 160 °C for two days. The ruthenium precursors $[(\eta^6\text{-}C_6H_6)RuCl_2]_2$ and $[(\eta^6\text{-}C_6H_5CF_3)RuCl_2]_2$ and all β-diketiminates were prepared according to literature procedures.[16,35,39,67−69] The corresponding β-diketiminato−lithium complexes were prepared by treating the appropriate protonated β-diketiminate dissolved in pentane with a stoiciometric quantity of n-BuLi (1.6 M in hexanes) at −70 °C.[40] The precipitated, highly air and moisture sensitive solids were collected and washed with small amounts of pentane. All other reagents were purchased from commercial sources and used as received. NMR spectra were recorded using either Bruker Avance 200 or 400 instruments. ^1H (COSY, NOE) and ^{13}C (HMBC and HSQC) one- and two-dimensional spectra were used to assign molecular connectivity and conformation in solution. Deuterated dichloromethane was distilled over CaH_2 and stored over 4 Å molecular sieves. Chemicals shifts for ^1H and ^{13}C spectra were referenced to Me_4Si, and ^{19}F spectra were referenced to CF_3Cl. ATR FT-IR spectra were recorded on a Perkin-Elmer Spectrum-One instrument using freshly ground samples pressed on top of a diamond anvil window. Sample preparation and spectral recording (in air) were performed within 2 min. Elemental microanalyses were obtained using an Exeter Analytical CE-440 elemental analyzer. Mass spectra were recorded using either electrospray or nanoelectrospray techniques on a ThermoFinnigan LCQ DECA XP Plus quadrupole ion trap instrument set in positive mode (flow rate: 5 μL per min; spray voltage: 5 kV; capillary temperature: 100 °C; capillary voltage: 20 V). Conditions were used as described previously.[70] Spectrophotometric measurements were performed in a 9:1 solution of methanol/water in quartz Suprasil curvettes (1 cm path length) on either a Perkin-Elmer Lambda 850 or a Jasco V-550 spectrometer at 25 °C.

Synthesis of $(\eta^6\text{-}C_6H_6)RuCl[(C_6H_5NC(CH_3)]_2CH$, 7. To a 50 mL Schlenk flask was added 0.125 g of $[(\eta^6\text{-}C_6H_6)RuCl_2]_2$ (orange powder) along with CH_2Cl_2 (10 mL). Subsequently, 2 equiv of the corresponding β-diketiminato−lithium complex $Li[(C_6H_5NC(CH_3)]_2CH$ (0.142 g, 0.507 mmol) was dissolved in 10 mL of CH_2Cl_2. This solution was slowly added to the reaction mixture over a period of approximately 0.5 h. The flask was capped, and the reaction mixture was stirred for 14 h. Afterward, the resulting dark red or purple solution was filtered through a 1 cm Celite−Schlenk frit combination, and the solution was reduced under vacuum to a volume of ca. 1 mL. While stirring, 25 mL of pentane was added, causing the formation of a purple or red precipitate. This solid was collected on a Schlenk frit and washed three times with 5 mL of *n*-pentane. For recrystallization, the complex was dissolved in a minimum amount of acetone or chloroform, and *n*-pentane was slowly added until the majority of the compound had crystallized. This purple microcrystalline solid was filtered and washed with

(57) Nguyen, A.; Top, S.; Pigeon, P.; Vessieres, A.; Hillard, E. A.; Plamont, M. A.; Huche, M.; Rigamonti, C.; Jaouen, G. *Chem.−Eur. J.* **2009**, *15* (3), 684–696.
(58) Top, S.; Thibaudeau, C.; Vessières, A.; Brulé, E.; Le Bideau, F.; Joerger, J.-M.; Plamont, M.-A.; Samreth, S.; Edgar, A.; Marrot, J.; Herson, P.; Jaouen, G. *Organometallics* **2009**, *28* (5), 1414–1424.
(59) Strohfeldt, K.; Tacke, M. *Chem. Soc. Rev.* **2008**, *37* (6), 1174–1187.
(60) Hogan, M.; Claffey, J.; Pampillon, C.; Tacke, M. *Med. Chem.* **2008**, *4* (2), 91–99.
(61) Kirin, S. I.; Ott, I.; Gust, R.; Mier, W.; Weyhermuller, T.; Metzler-Nolte, N. *Angew. Chem., Int. Ed.* **2008**, *47* (5), 955–959.
(62) Gross, A.; Metzler-Nolte, N. *J. Organomet. Chem.* **2009**, *694* (7−8), 1185–1188.
(63) Zobi, F.; Blacque, O.; Sigel, R. K. O.; Alberto, R. *Inorg. Chem.* **2007**, *46* (25), 10458–10460.
(64) Xavier, C.; Giannini, C.; Gano, L.; Maiorana, S.; Alberto, R.; Santos, I. *J. Biol. Inorg. Chem.* **2008**, *13* (8), 1335–1344.
(65) Romerosa, A.; Saoud, M.; Campos-Malpartida, T.; Lidrissi, C.; Serrano-Ruiz, M.; Peruzzini, M.; Garrido, J. A.; Garcia-Maroto, F. *Eur. J. Inorg. Chem.* **2007**, (18), 2803–2812.
(66) Shriver, D. F.; Drezdzon, M. A., *The Manipulation of Air-Sensitive Compounds*, 2nd ed.; Wiley-Interscience: Weinheim, 1986.
(67) Bennett, M. A.; Smith, A. K. *J. Chem. Soc., Dalton Trans.* **1974**, *2*, 233–241.
(68) Gao, W.; Mu, Y.; Li, G.-H.; Liu, X.-M.; Su, Q.; Yao, W.; Feng, S.-H. *Gaodeng Xuexiao Huaxue Xuebao* **2005**, *26* (1), 134–137.
(69) Budzelaar, P. H. M.; De Gelder, R.; Gal, A. W. *Organometallics* **1998**, *17* (19), 4121–4123.
(70) Dyson, P. J.; McIndoe, J. S. *Inorg. Chim. Acta* **2003**, *354*, 68–74.

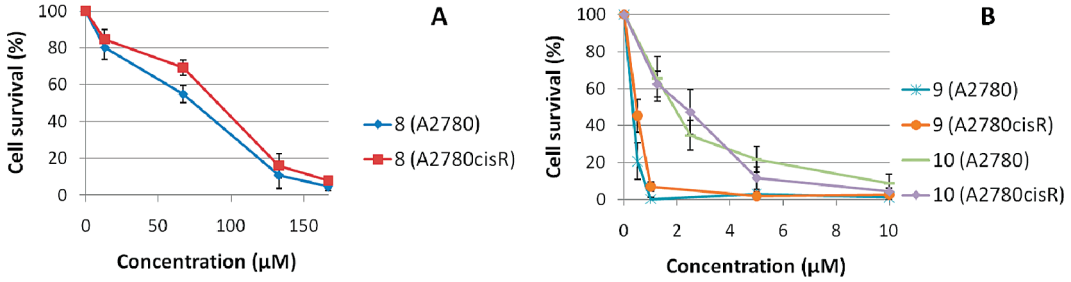

Figure 6. Cell viability using the MTT test: (A) viability of A2780 and A2780cisR cells after 72 h of incubation with **8**; (B) viability of A2780 and A2780cisR cells after 72 h of incubation with **9** and **10**.

10 mL of *n*-pentane and dried for at least 10 h under high vacuum, yield 0.159 g (0.336 mmol, 67.3%). Spectroscopic analysis reveals residual CH_2Cl_2 is present. Anal. Calcd for **7**: C, 59.54; H, 5.00; N, 6.04. Found: C, 58.52; H, 4.94; N, 5.91. ESI-MS (25 °C, dry CH_2Cl_2), (*m*/*z*) positive mode: 429.0 ([M − Cl − H]$^+$ 60%, calcd 429.1), 351.1 ([M − H − Cl − C_6H_6], 40%, calcd 351.0). ^{1}H NMR (25 °C, 400.1 MHz, CD_2Cl_2) δ(ppm): 1.65 (s, 6H, α-CH_3), 4.45 (s, 1H, *β*-C*H*), 4.52 (s, 6H, η^6-C_6H_6), 7.40 (m, $^3J_{HH}$ = 7.46 Hz, 4H, Ar *o*-C*H*), 7.46 (m, $^3J_{HH}$ = 7.45 Hz, 2H, Ar *p*-C*H*), 7.63 (m, $^3J_{HH}$ = 7.45, $^3J_{HH}$ = 7.46, 4H, Ar *m*-C*H*). ^{13}C NMR (25 °C, 100.1 MHz, CD_2Cl_2) δ(ppm): 24.69 (s, α-*C*H$_3$), 86.32 (s, η^6-*C*$_6$H$_6$), 94.42 (s, *β*-*C*H), 125.24 (s, Ar *p*-*C*H), 126.92 (s, Ar *m*-CH), 127.63 (s, Ar *m*-*C*H), 129.68 (s, Ar *o*-*C*H), 159.85 (s, α-C*C*H$_3$), 160.12 (s, Ar *i*-*C*). FT-IR (25 °C, solid): ν(cm^{-1}): 3391(br), 3056(w), 2922(w), 1590(w), 1558(m), 1529(m), 1482(m), 1457(s), 1432(m), 1401(s), 1349(w), 1277(w), 1203(m), 1164(w), 1152(w), 1136(w), 1070(w), 1039(w), 1033(w), 1022(w), 977(w), 955(w), 922(w), 884(w), 860(w), 844(w), 821(m), 821(m), 760(m), 753(m), 712(s), 704(s), 665(w).

Synthesis of (η^6-C_6H_6)RuCl((3,5-$(CF_3)_2C_6H_3NC(CH_3)$)$_2$CH, 8. The magenta-colored complex was prepared using a method identical to that employed for complex **7**. [(η^6-C_6H_6)$RuCl_2$]$_2$ (0.125 g, orange powder) and 0.280 g (0.507 mmol) of Li ((3,5-$(CF_3)_2C_6H_3NC(CH_3)$)$_2$CH (white powder) were used. Yield of **8**: 0.298 g (0.392 mmol, 78.5%). Spectroscopic analysis reveals residual CH_2Cl_2 is present. Anal. Calcd for **8**: C, 44.06; H, 2.60; N, 3.81. Found: C, 44.94; H, 2.51; N, 3.59. ESI-MS (25 °C, CH_2Cl_2), (*m*/*z*) positive mode: 700.9 ([M − Cl − H]$^+$, 100%, calcd 701.0). ^{1}H NMR (25 °C, 400.1 MHz, CD_2Cl_2) δ(ppm): 1.65 (s, 9H, α-CH_3), 4.45 (s, 1H, *β*-C*H*), 4.52 (s, 6H, η^6-C_6H_6), 8.06 (s, 2H, Ar *p*-CH), 8.15 (s, 4H, Ar *o*-CH). ^{13}C NMR (25 °C, 100.6 MHz, CD_2Cl_2) δ(ppm): 24.68 (s, α-*C*CH$_3$), 86.30 (s, η^6-C_6H_6), 94.41 (s, *β*-*C*H), 123.18 (q, $^1J_{CF}$ = 316 Hz, Ar *C*F$_3$), 125.24 (s, Ar *p*-*C*H), 126.90 (s, Ar *o*-*C*H), 129.03 (s, Ar *o*-*C*H'), 133.19 (q, $^2J_{CF}$ = 34.0 Hz, Ar *m*-*C*CF$_3$), 159.82 (s, Ar *i*-*C*), 160.10 (s, α-*C*CH$_3$). ^{19}F NMR (25 °C, 188.1 MHz, CD_2Cl_2) δ(ppm): −59.2 (s, $^1J_{FC}$ = 316 Hz, 3,5-$(CF_3)_2C_6H_3$). FT-IR (25 °C, solid): 3401(br w), 1618(w), 1558(w), 1536(m), 1456(m), 1437(w), 1401(w), 1359(s), 1275(s), 1223(w), 1167(s), 1127(s), 1114(s), 1039(w), 1010(w), 985(m), 938(w), 930(w), 915(w), 895(m), 873(w), 845(w), 823(m), 768(w br), 717(w), 703(m), 682(s).

Synthesis of (η^6-C_6H_6)RuCl((2,6-$(CH_3)_2C_6H_3NC(CF_3)$)$_2$CH, 9. The dark pink colored compound was prepared using an identical method to that for complex **7**. [(η^6-C_6H_6)$RuCl_2$]$_2$ (0.125 g, 0.500 mmol) (orange powder) with 0.210 g (0.500 mmol) of Li((2,6-$(CH_3)_2C_6H_3NC(CF_3)$)$_2$CH was employed. Yield: 0.246 g (0.392 mmol, 78.4%). Anal. Calcd for **9**: C, 51.64; H, 4.01; N, 4.46. Found: C, 51.08; H, 3.93; N, 4.40. ESI-MS (25 °C, CH_2Cl_2), (*m*/*z*) positive mode: 701.1 ([M − Cl]$^+$, 100%, calcd 701.0). ^{1}H NMR (25 °C, 400.1 MHz, CD_2Cl_2) δ(ppm): 2.52 (br s, 6H, *o*-CH_3), 4.59 (s, 6H, η^6-C_6H_6), 5.55 (s, 1H, *β*-C*H*), 7.52 (m, 6H, Ar *m*-,*p*-CH). ^{13}C NMR (25 °C, 100.1 MHz, CD_2Cl_2) δ(ppm): 19.66 (s, Ar *o*-*C*H$_3$), 87.93 (s, 6H, η^6-C_6H_6), 90.93 (s, *β*-*C*H), 119.44 (q, $^1J_{CF}$ = 283 Hz, α-*C*F$_3$), 127.01 (s, Ar *p*-*C*H), 128.75 (s, Ar *m*-*C*H), 133.86 (s, Ar *o*-*C*), 151.35 (q, $^2J_{CF}$ = 30.93 Hz, α-*C*CF$_3$)$_3$), 154.12 (s, Ar *i*-*C*). ^{19}F NMR (25 °C, 188.1 MHz, CD_2Cl_2) δ(ppm): −64.2 (s, $^1J_{FC}$ = 283 Hz, α-C*F*$_3$). FT-IR (25 °C, solid) ν(cm^{-1}): 3183(w), 3060(w), 3008(w), 2928(w), 1593(w), 1570(w), 1551(w), 1471(m), 1455(m), 1384(w), 1311(m), 1298(m), 1268(w), 1256(w), 1215(m), 1206(s), 1168(s), 1138(s), 1093(s), 1035(w), 1011(w), 982(w), 958(m), 920(w), 888(w), 833(s), 796(w), 768(s), 737(m), 715(w), 709(w), 692(w), 666(w).

Synthesis of (η^6-C_6H_6)RuCl((3,5-$(CF_3)_2C_6H_3NC(CF_3)$)$_2$CH, 10. This intense red colored compound was prepared with a method identical to that used for complex **7**. [(η^6-C_6H_6)$RuCl_2$]$_2$ (0.125 g, 0.500 mmol) (orange powder) with 0.321 g (0.504 mmol) of Li((3,5-$(CF_3)_2C_6H_3NC(CF_3)$)$_2$CH was employed. Anal. Calcd for **10**: C, 38.43; H, 1.55; N, 3.32. Found: C, 39.06; H, 1.84; N, 3.24. ESI-MS (25 °C, CH_2Cl_2), (*m*/*z*) positive mode: 809.0 ([M − Cl − H]$^+$, 77%, calcd 809.0), 730.9 ([M − C_6H_6 − Cl − H]$^+$, 23%, calcd 730.9). ^{1}H NMR (25 °C, 400.1 MHz, CD_2Cl_2) δ(ppm): 4.70 (s, 6H, η^6-C_6H_6), 5.54 (s, 1H, *β*-C*H*), 7.90 (s, 2H, Ar *p*-CH), 8.07 (s, 4H, Ar *o*-CH). ^{13}C NMR (25 °C, 100.6 MHz, CD_2Cl_2) δ(ppm): 86.96 (s, η^6-C_6H_6), 86.90 (s, *β*-*C*H), 119.07 (q, $^1J_{CF}$ = 285 Hz, α-*C*F$_3$), 120.09 (q, $^3J_{CF}$ = 3.69 Hz, Ar *p*-*C*H), 122.99 (q, $^1J_{CF}$ = 258 Hz, Ar *m*-*C*F$_3$), 126.43 (s, Ar *o*-*C*H), 131.63 (m, $^2J_{CF}$ = 33.9 Hz, Ar *m*-*C*CF$_3$), 150.85 (q, $^2J_{CF}$ = 26.9 Hz, α-*C*CF$_3$), 156.52 (s, Ar *i*-*C*). ^{19}F NMR (25 °C, 188.1 MHz, CD_2Cl_2) δ(ppm): −63.7 (s, $^1J_{FC}$ = 258 Hz, Ar *m*-C*F*$_3$), −59.7 (s, $^1J_{FC}$ = 285 Hz, α-C*F*$_3$). FT-IR (25 °C, solid) ν(cm^{-1}): 2160(w), 1584(w), 1558(w), 1466(m), 1364(s), 1312(w), 1277(s), 1222(m), 1172(s), 1132(s), 1117(s), 1104(s), 1011(w), 983(w), 962(m), 938(w), 900(m), 894(m), 874(m), 829(m), 805(w), 779(m), 743(w), 722(m), 708(m), 682(s).

Synthesis of {η^6-1,4-$CF_3C_6H_5$[2,6-$(CH_3)_2C_6H_3NC(CH_3)$]$_2$-CH}Ru[2,6-$(CH_3)_2C_6H_3NC(CH_3)$]$_2$CH, 11. In a 50 mL Schlenk flask, 0.200 g of [(η^6-$C_6H_5CF_3$)$RuCl_2$]$_2$ (orange powder) was dissolved in 25 mL of CH_2Cl_2. Two equivalents of the *β*-diketiminato−lithium complex Li((2,6-$(CH_3)_2C_6H_3NC(CH_3)$)$_2$CH was dissolved in 10 mL of CH_2Cl_2 and slowly added to the reaction mixture over a period of approximately 10 min. The flask was capped and the reaction mixture stirred for 36 h. Afterward, the resulting pink-colored solution was filtered through a 1 cm Celite−Schlenk frit combination, and the solvent removed under vacuum to dryness. The resulting residue was extracted with 30 mL of pentane and filtered through a 1 cm Celite−Schlenk frit combination. Slow evaporation of a saturated pentane solution in a glovebox resulted in the deposition of pink crystals. The remaining solution was decanted, and the product was dried for at least 2 h under high vacuum, yield 42%. The compound is highly sensitive to oxygen. Anal. Calcd for **11**: C, 68.59; H, 6.46; N, 6.53. Found: C, 67.82; H, 6.40; N, 6.44. Atom labels for the NMR assignment of **11** are given in Figure 7. ^{1}H NMR (25 °C, 400.1 MHz, C_6D_6) δ(ppm): 1.45 (s, 6H, *m*-CH_3), 1.70 (s, 6H, α-CH_3), 1.93 (s, 6H, *b*-CH_3), 2.02 (s, 6H, *f*-CH_3), 2.25 (s, 6H, *n*-CH_3), 2.37 (s, 6H, *r*-CH_3), 2.72 (d, $^3J_{HH}$ = 10.7 Hz, *k*-C*H*), 2.81 (dd, $^3J_{HH}$ = 6.48 Hz, $^3J_{HH}$ = 6.30 Hz, 2H, *i*-C*H*), 3.45 (dd, $^3J_{HH}$ = 6.30 Hz, $^3J_{HH}$ = 10.7 Hz, 1H, *j*-C*H*), 3.49 (d, $^3J_{HH}$ = 6.48 Hz, 2H, *h*-C*H*), 5.47 (s, 1H, *β*-C*H*), 7.04 (m, 8H, *d*-,*o*-,*p*-,*r*-C*H*), 7.13 (m, 2H, *e*-C*H*), 7.19 (m, 2H, *c*-C*H*). ^{13}C

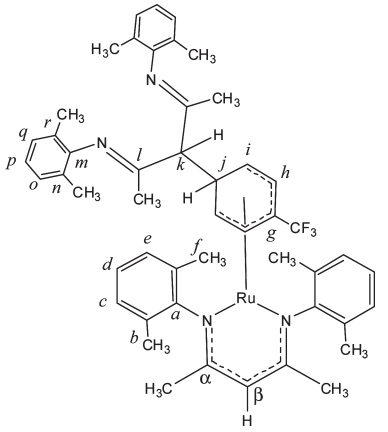

Figure 7. Labeling diagram for the positions of hydrogen and carbon atoms in complex **11**.

NMR (25 °C, 100.1 MHz, C_6D_6) δ(ppm): 18.09 (s, *n*-CH_3), 18.63 (s, *b*-CH_3), 18.77 (s, *f*-CH_3), 18.89 (s, *l*-CH_3), 19.00 (s, *r*-CH_3), 22.82 (s, α-CH_3), 40.50 (s, *j*-CH), 47.35 (s, *i*-CH), 70.73 (s, *k*-CH), 73.59 (s, *h*-CH), 80.49 (q, $^2J_{CF}$ = 35.4 Hz, *g*-CH), 100.25 (s, β-CH), 122.87 (s, *p*-CH), 124.84 (s, *f*-CCH_3), 125.34 (s, *q*-CH), 125.37 (s, *o*-CH), 127.68 (s, *b*-CCH_3), 128.08 (s, *d*-CH), 128.13 (s, *c*-CH), 128.28 (s, *e*-CH), 129.64 (s, *r*-CCH_3), 130.65 (q, $^1J_{CF}$ = 271 Hz, CF_3), 132.22 (s, *n*-CCH_3), 149.28 (s, *a*-C), 154.03 (s, *m*-C), 159.65 (s, α-CCH_3), 167.43 (s, *l*-CCH_3). ^{19}F NMR (25 °C, 188.1 MHz, CD_2Cl_2) δ(ppm): −60.2 (s, $^1J_{FC}$ = 271 Hz, CF_3). FT-IR (25 °C, Nujol mull) ν(cm^{-1}): 1652(m), 1624(w), 1594(w), 1541(m), 1521(w), 1319(m), 1286(w), 1262(w), 1248(w), 1209(w), 1185(m), 1166(m), 1159(m), 1118(m), 1092(w), 1053(w), 1030(w), 985(w), 961(w), 935(w), 919(w), 881(w), 853(w), 828(w), 798(w), 789(w), 722(w), 698(w), 689(w), 634(w), 621(w), 541(w).

Crystallographic Details. Suitable single crystals were removed from the sample vial under a flow of N_2 and manipulated in a perfluoropolyalkyl ether oil matrix (F06206K, ABCR company) in a specially constructed Dewar partially filled with liquid nitrogen. The crystals were mounted on the end of a glass fiber (diameter at least 0.1 mm) attached to a metal pin fixed to a goniometer head, which was placed in the Euler cradle, while maintaining a cold blanket of N_2 gas. For structures **7**−**9** and **11**, a Nonius Kappa-CCD diffractometer equipped with a Bruker-Apex II CCD area detector and an Enraf-Nonius FR590 X-ray generator was used, while for **10**, an Oxford-Diffraction Kuma Kappa diffractometer with a Sapphire CCD area detector was employed. Both instruments utilize a graphite-monochromated Mo Kα radiation source with $\lambda = 0.71073$ Å. The crystals were kept under a 140 or 100 K gaseous flow of N_2 during the collection procedure. The unit cell and orientation matrix were determined by indexing reflections measured from phi−chi scans and analyzed with the program DIRAX,[71,72] or in the case of **10** the unit cell was determined from the entire data set using CrysAlis RED.[73] All data sets are based on collecting reflections using an optimized scanning strategy utilizing the programs CollectCCD and CrysAlis CCD (for **10** only).[74] After data integration with either EvalCCD[75] or CrysAlis RED (for **10** only),[73] a multiscan absorption correction based on a semiempirical method was applied using the SADABS[8] or ABSSCALE program in CrysAlis RED.[73] Space group determination was performed with the XPREP program.[76] A structure solution based on the direct-method algorithm was employed with SHELXS-97.[77] Afterward, anisotropic refinement of all non-hydrogen atoms was completed on the basis of a least-squares full-matrix method against F^2 data using SHELXL-97.[77] Hydrogen atoms were added through geometrically calculated positions and refined as a riding model using a scaled thermal parameter to the connecting atom. In structures **8** and **9**, a positional η^6-ring was treated by splitting the atoms over two positions, the indivdual occupancy of the disordered groups were allowed to freely refine, while the total site occupancy was set to 1.0 (details described in the accompanying CIFs). A similar procedure was employed for the disordered η^5-cyclohexadienyl β-diimine component in complex **11**. A small number of reflections in some cases were removed when $\Delta(F_o^2 - F_c^2)/\sigma$ exceeded 10.0. Selected crystallographic data for all structures are given in the Supporting Information. Drawings were produced with the program ORTEP-3.[78]

Computational Studies. In silico studies were performed using the Gaussian 03 program[79] employing density functional theory with the three-parameter hybrid B3LYP method, which incorporates the exchange functional developed by Lee, Parr, and Yang.[80,81,82] For all nonmetal atoms, the contracted 6-31G(d,p) basis set was selected, which includes diffuse functions.[83] For the ruthenium center, the double-ζ basis set, LANL2dz, was used in conjunction with a pseudopotential representing the core set of electrons.[84] All structures were geometrically optimized to an energy minimum. The position on the local potential energy surface was confirmed through vibration analysis using second derivatives, where no imagery frequencies were observed. The electrostatic potential maps were generated from the calculated electron density using Gaussview 3.[85]

Cells and Cell Treatment. Human A2780 and A2780cisR cells were obtained from the European Centre of Cell Cultures (ECACC, Porton down, Salisbury, UK). All cell culture reagents were obtained from Gibco-BRL (Basel, Switzerland). The cells were grown in RPMI 1640 medium containing 10% fetal calf serum (FCS) and antibiotics. The complexes were dissolved in DMSO as 40 mM for stock solution and then diluted in complete medium to the required concentration. DMSO at comparable concentrations did not show any effects on cell cytotoxicity (results not shown).

(71) Duisenberg, A. J. M. *J. Appl. Crystallogr.* **1992**, *25*, 92–96.
(72) Duisenberg, A. J. M.; Hooft, R. W. W.; Schreurs, A. M. M.; Kroon, J. *J. Appl. Crystallogr.* **2000**, *33* (2), 893–898.
(73) *CrysAlis Pro RED, 1.71*; Oxford Diffraction Ltd.: Yarnton, Oxfordshire, U.K., 2006.
(74) *CrysAlis Pro CCD, 1.71*; Oxford Diffraction Ltd.: Yarnton, Oxfordshire, U.K., 2006.
(75) Duisenberg, A. J. M.; Kroon-Batenburg, L. M. J.; Schreurs, A. M. M. *J. Appl. Crystallogr.* **2003**, *36*, 220–229.
(76) Sheldrick, G. M. *XPREP, A Reciprocal Space Exploration Program, 2.06*; Bruker-AXS: Madison, WI, 2003.
(77) Sheldrick, G. *Acta Crystallogr., Sect. A* **2008**, *64* (1), 112–122.
(78) Farrugia, L. *J. Appl. Crystallogr.* **1997**, *30* (5 Part 1), 565.
(79) Frisch, M. J. T., G. W.; Schlegel, H. B.; Scuseria, G. E.; Robb, M. A.; Cheeseman, J. R.; Montgomery, J. A., Jr.; Vreven, T.; Kudin, K. N.; Burant, J. C.; Millam, J. M.; Iyengar, S. S.; Tomasi, J.; Barone, V.; Mennucci, B.; Cossi, M.; Scalmani, G.; Rega, N.; Petersson, G. A.; Nakatsuji, H.; Hada, M.; Ehara, M.; Toyota, K.; Fukuda, R.; Hasegawa, J.; Ishida, M.; Nakajima, T.; Honda, Y.; Kitao, O.; Nakai, H.; Klene, M.; Li, X.; Knox, J. E.; Hratchian, H. P.; Cross, J. B.; Bakken, V.; Adamo, C.; Jaramillo, J.; Gomperts, R.; Stratmann, R. E.; Yazyev, O.; Austin, A. J.; Cammi, R.; Pomelli, C.; Ochterski, J. W.; Ayala, P. Y.; Morokuma, K.; Voth, G. A.; Salvador, P.; Dannenberg, J. J.; Zakrzewski, V. G.; Dapprich, S.; Daniels, A. D.; Strain, M. C.; Farkas, O.; Malick, D. K.; Rabuck, A. D.; Raghavachari, K.; Foresman, J. B.; Ortiz, J. V.; Cui, Q.; Baboul, A. G.; Clifford, S.; Cioslowski, J.; Stefanov, B. B.; Liu, G.; Liashenko, A.; Piskorz, P.; Komaromi, I.; Martin, R. L.; Fox, D. J.; Keith, T.; Al-Laham, M. A.; Peng, C. Y.; Nanayakkara, A.; Challacombe, M.; Gill, P. M. W.; Johnson, B.; Chen, W.; Wong, M. W.; Gonzalez, C.; and Pople, J. A. *Gaussian 03, Revision E.01*; Gaussian Inc.: Wallingford CT, 2004.
(80) Becke, A. D. *J. Chem. Phys.* **1993**, *98* (7), 5648–5652.
(81) Vosko, S. H.; Wilk, L.; Nusair, M. *Can. J. Phys.* **1980**, *58* (8), 1200–1211.
(82) Stephens, P. J.; Devlin, F. J.; Chabalowski, C. F.; Frisch, M. J. *J. Phys. Chem.* **1994**, *98* (45), 11623–11627.
(83) Petersson, G. A.; Allaham, M. A. *J. Chem. Phys.* **1991**, *94* (9), 6081–6090.
(84) Hay, P. J.; Wadt, W. R. *J. Chem. Phys.* **1985**, *82* (1), 299–310.
(85) *Gaussview, 3*; Gaussian Inc.: Wallingford, CT, 2003.

Determination of Cytotoxicity. Cells were grown in 96-well cell culture plates (Corning, NY) at the density of ca. 25×10^3 cells per well. The culture medium was replaced with fresh medium containing complexes **8**−**10** at concentrations varying respectively from 0 to 160 μM for **8** and from 0 to 10 μM for **9** and **10**, with an exposure time of 72 h. Thereafter, the medium was replaced by fresh medium, and cell survival was measured using the MTT test as previously described.[86] Briefly, 3-(4,5-dimethyl-2-thiazoyl)-2,5-diphenyltetrazolium bromide (MTT, Merck) was added at 250 μg/mL, and incubation was continued for 2 h. Then the cell culture supernatants were removed, the cell layer was dissolved in DMSO, and absorbance at 540 nm was measured in a 96-well multiwell plate reader (iEMS Reader MF, Labsystems, Bioconcept, Switzerland) and compared to the values of control cells incubated without complexes. Experiments were conducted in quadruplicate wells and repeated at least twice.

(86) Berger, Y.; Greppi, A.; Siri, O.; Neier, R.; Juillerat-Jeanneret, L. *J. Med. Chem.* **2000**, *43* (25), 4738–4746.

Acknowledgment. This research was supported by grants from the European Commission Marie Curie Action (A.D.P., MEIF-CT-2005-025287, CARCAS; A. A.N., MEIF-CT-220890-SuRuCo), the Swiss National Science Foundation, the EPFL (A.D.P., O.Z., A.A.N., and P.J.D.), and University College Dublin. A.D.P. thanks Science Foundation Ireland (SFI) for a Stokes Lectureship. Computational resources were provided by the Irish Center for High-End Computing (ICHEC), Dublin, Ireland.

Supporting Information Available: This material is available free of charge via the Internet at http://pubs.acs.org.